



Correlations between creep parameters and application to probabilistic damage assessments



N.A. Zentuti*, J.D. Booker, R.A.W. Bradford, C.E. Truman

Solid Mechanics Research Group, University of Bristol, Queens Building, University Walk, Bristol, BS8 1TR, United Kingdom

ARTICLE INFO

Keywords:
Creep
Damage
Correlations
Sensitivity analysis
Monte-Carlo
Probabilistic

ABSTRACT

This work formalises an approach for identifying and implementing correlations in probabilistic creep crack initiation assessments. The methodology is based on partitioning data obtained from uniaxial creep test results into subsets according to temperature and stress. This work is focused on 316H stainless steel and is concerned with identifying correlations between creep deformation, creep ductility and rupture life. However, the methodology can be implemented to identify correlations for any material and any combination of properties. An implementation method is also presented for sampling correlated parameters in Monte-Carlo simulations using the Spearman rank order correlation. This is followed by a discussion of the key effects that incorporating correlations might have on probabilistic creep damage results. While a degree of correlation between ductility and creep deformation exists, it was found to be uncertain. Conducting post-assessment sensitivity analyses based on uncorrelated parameters is suggested as a means for providing focus as to which correlations are most important for the assessment results.

1. Introduction

A crucial aspect of any probabilistic assessment is the statistical characterisation of uncertainties in the input parameters. These are commonly defined in terms of either *aleatory* uncertainties, characterised by chance or irreducible randomness in the data, or *epistemic* which arises from a lack of knowledge of the underlying mechanisms [1]. The overall uncertainty in a material property can therefore be considered as comprising of two parts: an aleatory component due to scatter within a given cast and an epistemic component due to cast-to-cast differences. The former are considered random variations, whilst the latter are typically due to subtle differences in chemical compositions or manufacturing processes. Inter-parameter correlations can also contribute to the overall uncertainty in the output result of a probabilistic calculation. The subject of incorporating correlations between creep parameters (e.g. creep strain rate and creep ductility [2]) is generally acknowledged for its importance, but not widely identified and addressed. For example, in Ref. [3] it is suggested that joint probability distributions can be used to sample correlated parameters, but this was expected to pose difficulties arising from the absence of rigorous statistical data treatment [4]. In Ref. [3] it is proposed that uncertainties can be quantified by dividing the available data into appropriate subsets from which statistical measures are inferred.

The application of interest involves conducting probabilistic analyses of creep crack initiation assessments (e.g. the calculation of creep damage outlined in the R5 Volume 2/3 assessment procedure [5] developed by EDF Energy). For such assessments, material properties are key sources of uncertainty, especially the creep related ones due to large scatter. Identifying and incorporating correlations can have a considerable, and often advantageous, effect on the predicted probability of failure (PoF). This work formalises a methodology for characterising and incorporating correlations between input parameters in probabilistic creep damage calculations. The results and discussion in this work are focused on 316H stainless steel, for which the required data was extracted from a materials testing database managed by EDF Energy. Correlations between creep ductility and creep deformation are of most interest, and were calculated based on uniaxial creep test results obtained from data subsets partitioned by applied temperature and stress. Following these calculations, an example driven discussion on how key correlations can affect probabilistic output results is presented.

2. Methodology

2.1. Uniaxial creep data

Most creep deformation and creep damage models are fitted to

* Corresponding author.

E-mail address: nz9512@bristol.ac.uk (N.A. Zentuti).

<https://doi.org/10.1016/j.ijpvp.2018.07.004>

Received 5 March 2018; Received in revised form 2 July 2018; Accepted 4 July 2018

Available online 07 July 2018

0308-0161/ © 2018 Elsevier Ltd. All rights reserved.

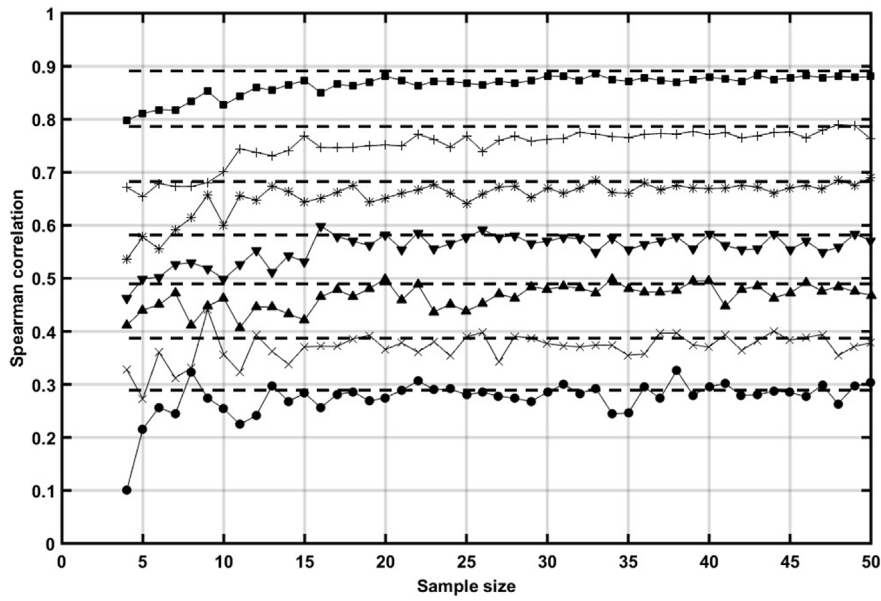


Fig. 1. A comparison for seven degrees of correlation (from 0.3 to 0.9) between the Spearman correlation coefficient as a function of sample size against correlations based on large populations (10^5 samples), the latter of which are represented by dashed lines. This shows that for smaller sample sizes the calculated coefficient deviates from the population coefficient.

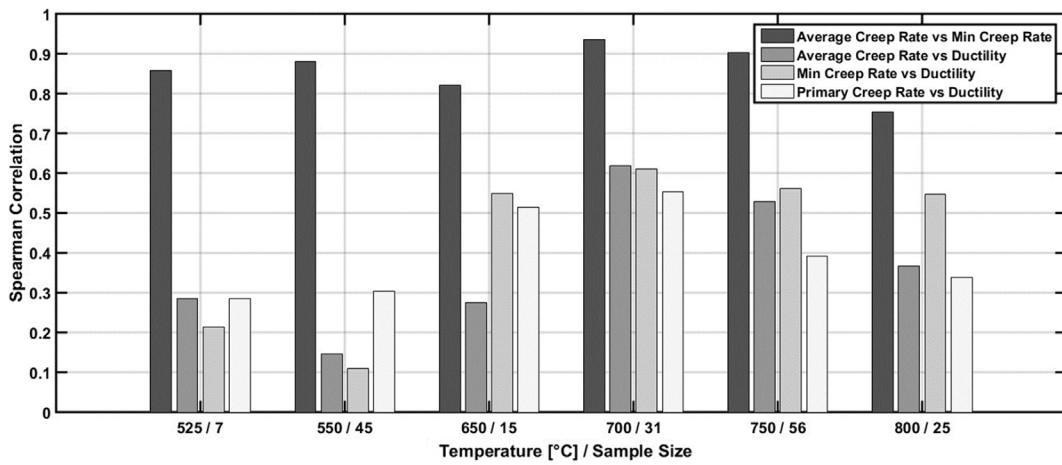


Fig. 2. Correlations between three measures of creep deformation and ductility (taken as ϵ_{LS}) based on temperature partitioned subsets.

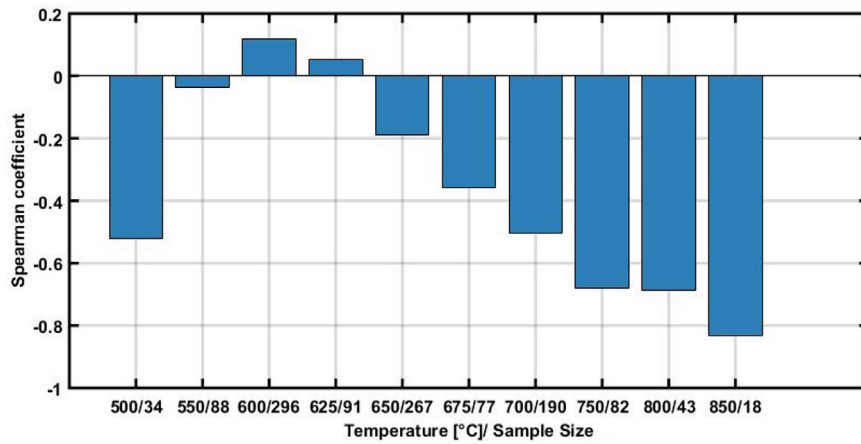


Fig. 3. Correlations between creep rupture time and creep ductility based on temperature partitioned subsets.

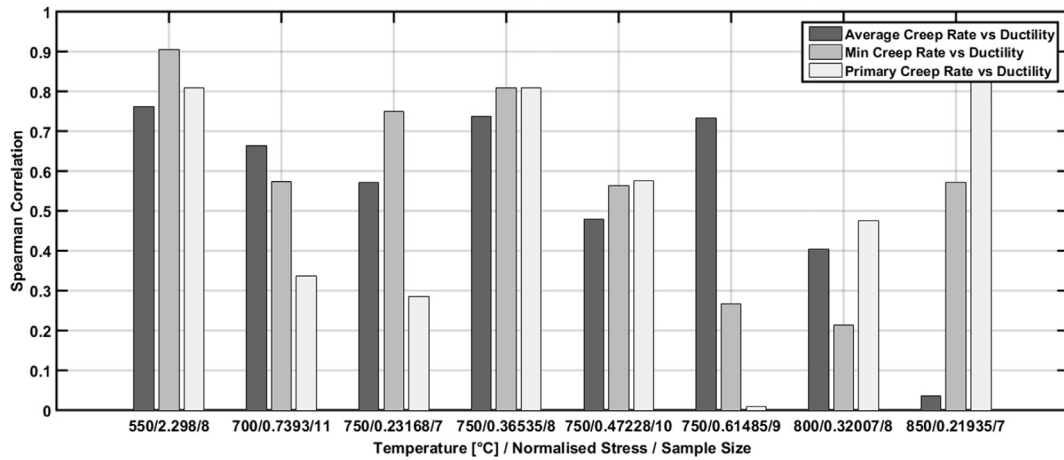


Fig. 4. Correlations between three measures of creep deformation and creep ductility (taken as ϵ_{LS}) based on temperature and stress partitioned subsets. The normalised stress is the applied stress over the temperature specific proof stress [14].

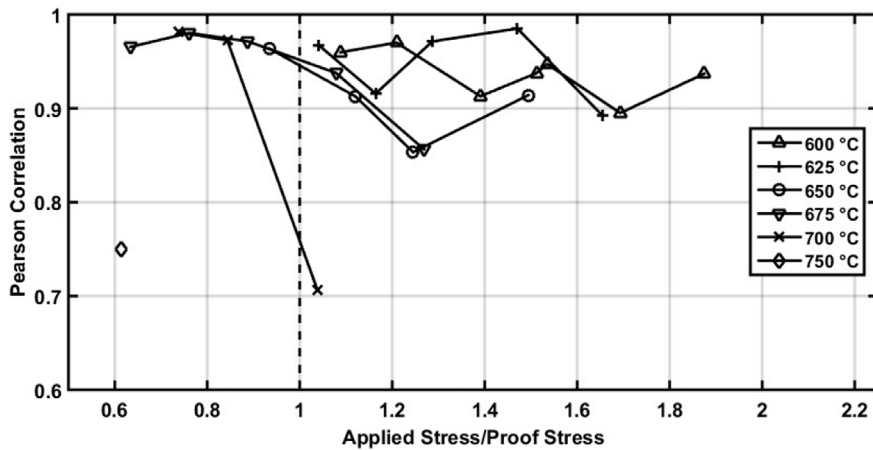


Fig. 5. Correlations between ϵ_{LS} and PRA based on temperature and stress partitioned subsets. Each subset has a minimum of 10 data points.

uniaxial creep rupture tests. It was therefore deemed appropriate to examine data sets from such tests to infer potential correlations between key creep parameters. Chosen due to their importance towards creep damage calculations, the parameters which were considered in this work are the following:

1. The uniaxial creep ductility, ϵ_f . Two measures of uniaxial ductility were available: the last recorded inelastic engineering strain (excluding any plastic strain introduced by the initial loading), ϵ_{LS} , and the percentage reduction of area at the necking point of the specimen (PRA).
2. The rupture time, t_R .
3. The average creep strain rate, $\dot{\epsilon}_A$, which was calculated as ϵ_{LS} over t_R .
4. The minimum (secondary) creep strain rate, $\dot{\epsilon}_S$. This was only available for 289 uniaxial creep tests within the database.
5. The primary creep strain rate coefficient, K . With the creep strain rate ($\dot{\epsilon}_p$) being variable during the primary stage of a creep test, K was chosen as an intermediary measure to characterise the primary deformation. The coefficient was based on the strain hardening version of the RCC-MR [6] model, thus it was calculated by fitting the creep strain rate data in the primary stage to the following expression:

$$\log(\dot{\epsilon}_p) = \log(K) + X \log(\epsilon_C) + Y \log(\sigma) \tag{1}$$

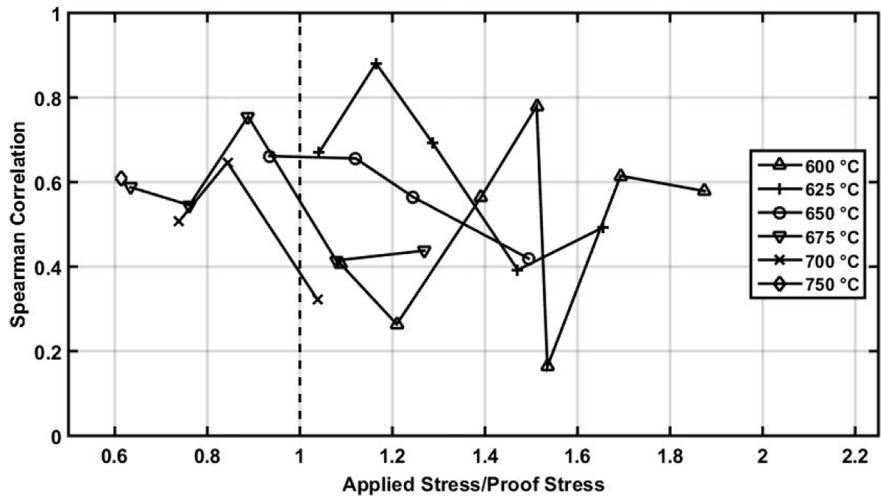
where ϵ_C is the instantaneous creep strain, and the creep constants X and Y were taken from Ref. [6].

It is worth noting that the data used in this work is based on

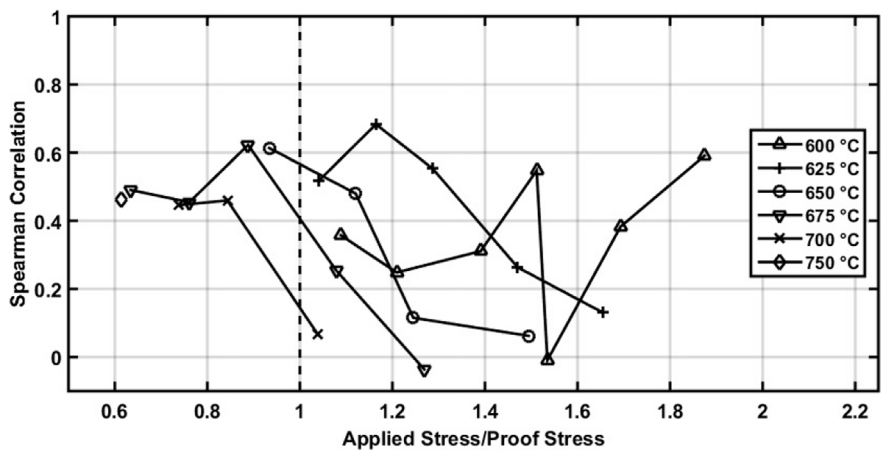
engineering stress and strain measurements.

The last recorded inelastic strain was the closest experimental recorded data to the desired uniaxial ductility that was available for all tests. The only other similar quantity was the percentage reduction of area. The former can be dependent on the rate of data recording whilst the latter is typically calculated based on room temperature measurements. Therefore, the inaccuracies in both ϵ_{LS} and PRA are considered epistemic uncertainties introduced by the experimental approach. It must be pointed out that the database included a vast array of tests that had been conducted over decades of research, and therefore finding a consistent measure that can be extracted from all tests was not always possible. This is a common problem in creep testing as strict consistency in conducting the tests and reporting the results is not always achievable across different laboratories at different times. Accordingly, the proposed approach for addressing this issue was to comparatively examine correlation between $\dot{\epsilon}_A$ and each of ϵ_{LS} and PRA. Effectively, together the two measures of ductility are used as surrogates in this work as ductility is not easily experimentally defined. As will be later discussed, this is especially compelling because last recorded inelastic strain and reduction of area are strongly correlated, which essentially implies that they are both proportional to the same quantity (i.e. ductility).

For primary creep, the aim was to find a single measure of creep rate per test. For some of the tests stress and strain were recorded during the test rather than just recording the last strain. Therefore the power law expression in Equation (1) was fitted to the stress-strain data recorded during each test. This raw creep strain data was only available for a



(a) $\dot{\epsilon}_A$ against ϵ_{LS}



(b) $\dot{\epsilon}_A$ against PRA

Fig. 6. Correlations between average creep rate and measures of uniaxial creep ductility based on temperature and stress partitioned subsets. The proof stress is temperature specific and was obtained from Ref. [14].

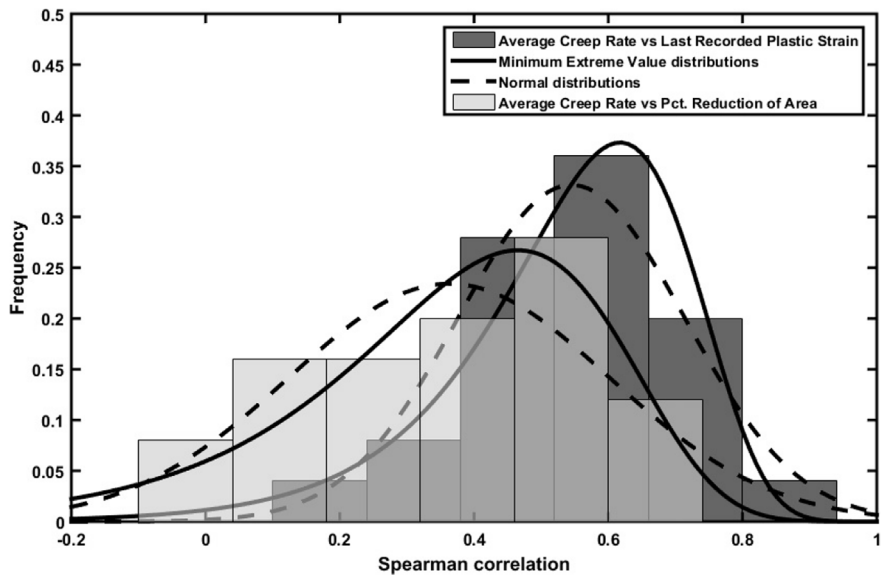


Fig. 7. Distribution fits to average creep rate versus ductility correlation results presented in Fig. 6.

Table 1
Fitted parameters for the distributions shown in Fig. 7.

Correlation	Distribution parameters			
	Normal		Minimum Extreme Value	
	μ	σ_D	ν	θ
$\dot{\epsilon}_A - \epsilon_{LS}$	0.545	0.168	0.618	0.138
$\dot{\epsilon}_A - PRA$	0.363	0.238	0.465	0.193

total of 289 uniaxial creep tests. For a single test it is not possible to fit three parameters at the same time. Thus by fixing two of the parameters at the values quoted in Ref. [7], for a single test a single value of K can be obtained. The purpose of this approach must not be confused with finding the optimal values of K , X and Y for 316H given all tests. Rather it attempts to encapsulate a measure of primary creep rate into a single value per test. This approach was driven by the limitation of the available data and the inherent uncertainty associated with characterising primary creep deformation.

The raw data for the creep parameters which was used in this work cannot be reproduced due to propriety issues. However, similar data plots for average creep rate, ductility and rupture time for 316H can be found in Ref. [7].

2.2. Data partitioning

Following the approach in Ref. [3], the available data was partitioned firstly by temperature only and then by both temperature and stress. Repeated tests using the same cast are rather rare and as a result it was not possible to correlate scatter in creep properties within specific casts. Repeats of the same test conditions, but for different casts were available, which are the focus of this work. Correlations between casts are believed to be more important as cast-to-cast variability typically dominates the uncertainty in creep test data. Cast-to-cast variabilities are typically attributed to marked or even subtle differences in chemical compositions, and in the case of Type 316 stainless steels these differences can produce large scatter in the creep properties [1]. Furthermore, when assessing populations of the same component for creep damage, it is often the case that these populations would comprise of a multitude of casts. This provides a further justification for basing this current work on datasets having multiple casts.

The main reason for partitioning the available data was to limit the effect of temperature and stress dependencies, thus isolating pure scatter in the data. Partitioning by either stress or temperature only would effectively introduce a misleading correlation that is driven by

the stress or temperature dependencies of the input parameters. This would in turn bias the correlations measured from the stress or temperature partitioned datasets. Therefore, it is advised that correlations obtained from data subsets partitioned by temperature alone must only be examined qualitatively. Furthermore, correlations from temperature and stress partitioned subsets are those advised to be used in probabilistic assessments. Whilst rigorous, a disadvantage of partitioning by both stress and temperature is the drastic reduction of the sample sizes from which meaningful correlations could be inferred.

2.3. Correlations

The Pearson correlation coefficient [8,9] is probably the most ubiquitous correlation statistic. It measures the strength of the linear relationship between two parameters. It also has a weak, and very often ignored, requirement that the parameters should be normally distributed. This is a parametric coefficient, since its expression includes the means of both parameters:

$$r = \frac{\sum_{i=1}^N (X_i - \bar{X})(Y_i - \bar{Y})}{\left(\sqrt{\sum_{i=1}^N (X_i - \bar{X})^2}\right)\left(\sqrt{\sum_{i=1}^N (Y_i - \bar{Y})^2}\right)} \tag{2}$$

where X_i and Y_i represent a data point, \bar{X} and \bar{Y} are the means and N is the total number of data points. The Spearman correlation, which is a non-parametric equivalent to Pearson's, determines the strength and direction of the monotonic relationship between two parameters [10]. It is calculated as the Pearson correlation between the ranks of the two sets of data being examined and is given by:

$$C_s = 1 - \frac{6 \sum_{i=1}^N d_i^2}{N(N^2 - 1)} \tag{3}$$

where d_i is the difference between the ranks assigned to each X_i and Y_i data pair. The value of C_s ranges from 0 to 1 (0 indicating no correlation and 1 indicating a perfect correlation), while its sign indicates whether the parameters are correlated or anti-correlated [8,10]. For the application presented here, the Spearman correlation was deemed to be more appropriate as it does not assume linearity (an assumption which may not apply for the parameters of interest) and is a non-parametric statistic which does not impose any *a priori* assumptions on the distributions of the input parameters. Therefore, parameters following different types of distributions can still be correlated using the Spearman correlation.

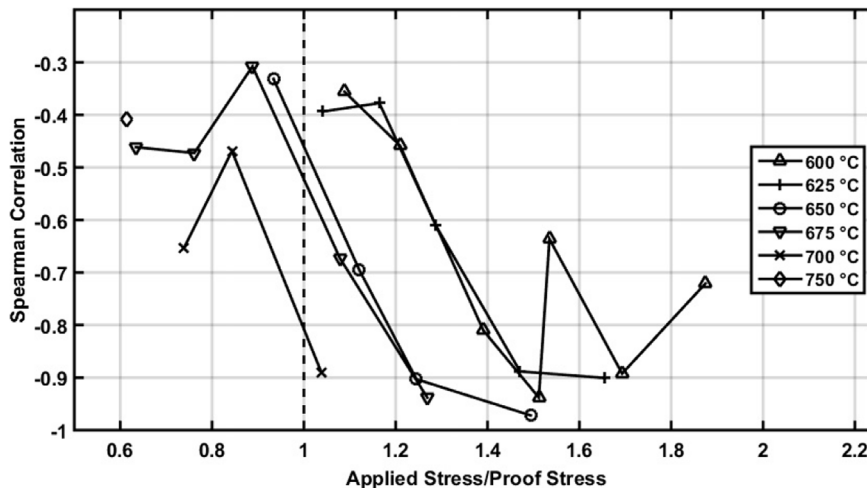


Fig. 8. Correlations between average creep rate and rupture time based on temperature and stress partitioned subsets. Each subset has a minimum of 10 data points.

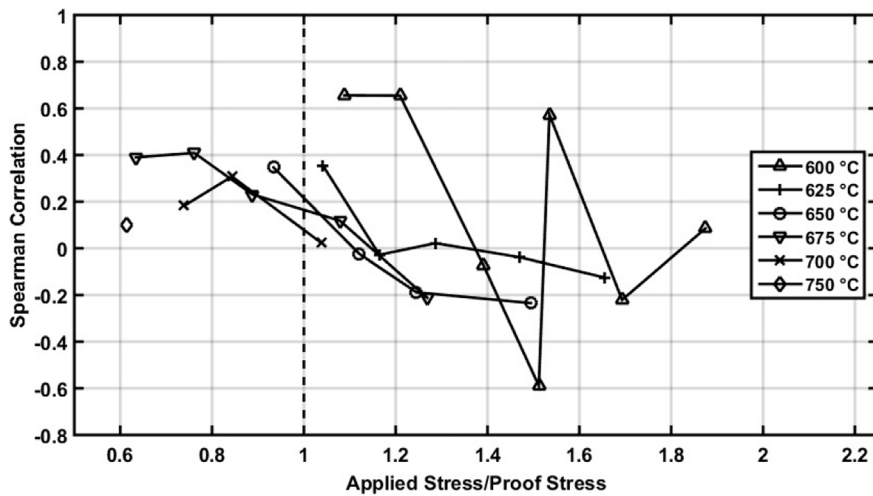


Fig. 9. Correlations between creep rupture time and uniaxial creep ductility based on temperature and stress partitioned subsets. Each subset has a minimum of 10 data points.

2.4. Sampling of correlated input parameters

A convenient and simple approach for producing sets of two correlated parameters is using a *Gaussian copula*. A detailed account of this method can be found in Ref. [11], whilst a practical example showing its implementation in MATLAB® can be found in Ref. [12]. The aim is to generate multivariate datasets with arbitrary probability density functions (PDFs) and Spearman correlations. The method involves two key steps to transform normally distributed, correlated datasets to ones which adhere to any arbitrary distribution. Furthermore, the random variables comprising the multivariate dataset do not have to necessarily follow the same type of distribution, thus providing a desirable degree of flexibility to this method. In Ref. [11] this procedure is termed *NORTA (NORMAL to Anything)* which in essence can be broken down into two steps:

1. Firstly a multivariate normal parameter (Z) is transformed into a multivariate uniform parameter U, in which case the distribution of U is known as a *copula*.
2. Secondly U is transformed into the desired multivariate parameter X, with its constituent variables having arbitrary cumulative distribution functions (CDFs). Thus the procedure is summarised in the following equation:

$$\mathbf{X} = \begin{bmatrix} F_{X_1}^{-1}[U_1] \\ F_{X_2}^{-1}[U_2] \\ \vdots \\ F_{X_k}^{-1}[U_k] \end{bmatrix} = \begin{bmatrix} F_{X_1}^{-1}[\Phi(Z_1)] \\ F_{X_2}^{-1}[\Phi(Z_2)] \\ \vdots \\ F_{X_k}^{-1}[\Phi(Z_k)] \end{bmatrix} \tag{4}$$

where Φ is the standard normal CDF and F_{X_i} is the desired CDF for the *i*th random variable.

2.5. Effect of sample size on correlations

A further important consideration is whether the sample size has an effect on the calculated correlation, and in turn how it affects the results of a probabilistic assessment which uses correlations based on relatively small data sets. The approach used to examine this effect was to produce two large (10^5 samples) sets of correlated parameters. Thereafter progressively smaller sets were obtained by randomly sampling from the large population set, and the associated correlations were calculated and compared with the correlation for the large population. The two parameters produced for this analysis were normally distributed and the Spearman correlation was used. Fig. 1 shows how reducing the

sample size causes a drift away from the correlations based on large populations, suggesting that for smaller data sets the correlations are usually smaller than those for the larger populations. However, this effect is not noticeable for sets larger than 30 data points. This effect can be rather considerable, and must be noted when correlations based on small data sets are used in probabilistic analyses.

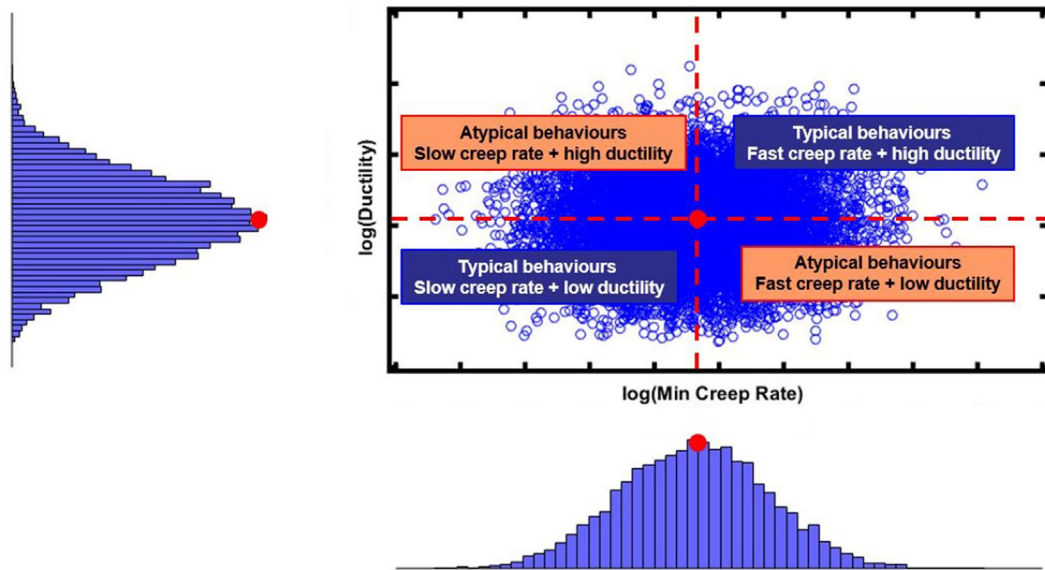
As to how this affects the probabilistic results, it solely depends on the nature of the probabilistic assessment and the degree of conservatism (or lack thereof) that comes with using a smaller correlation coefficient. As discussed in Section 4, for probabilistic creep damage assessments, a positive correlation between creep deformation and ductility yields a lower PoF. Thus a smaller positive correlation would increase the predicted PoF and thus has a conservative effect.

3. Results and discussion

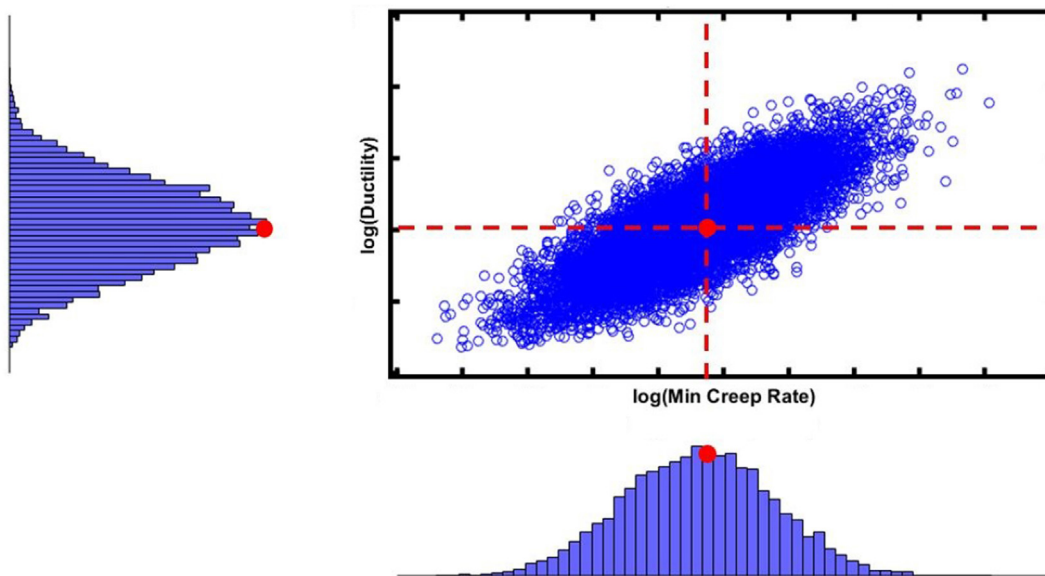
Figs. 2 and 3 show various correlations obtained for temperature partitioned data subsets. As previously discussed not partitioning by stress can have a marked effect on the calculated correlations and thus these results are not directly applicable to probabilistic assessments. However, it is worth noting that these results showed a changeover in correlations around 600°C. It is unclear what is the cause of this phenomenon but it may be related to a temperature induced failure mechanism change. For 316H it was previously observed that there is a trough around 500- 550°C in ductility when plotted as a function of temperature [13]. This might be linked with the effect in Fig. 3 as a manifestation of the creep ductility variation with temperature for 316H.

An important outcome, however, was that scatter in average and minimum creep rates appear to be strongly correlated, which was expected. This observation can be useful in the absence of enough raw data to calculate the minimum creep rate. The average creep rate data can be used as a proxy for inferring - not in absolute but rather in monotonic terms - the severity of scatter in the creep deformation data. Indeed it is believed that average and minimum creep rates should be near perfectly correlated, as they are both measures of the same phenomenon i.e. creep deformation. However, it is thought that some uncertainty was introduced by the data manipulations required for calculating these quantities from the raw test data.

The more important results are depicted in Figs. 4–7, which are based on data subsets partitioned by both temperature and stress. These show that consistently positive correlations between ductility (taken as the $\epsilon_{L,S}$) and various measures of creep deformation exist, albeit the exact values of these positive correlations are uncertain. Results for



(a) Uncorrelated.



(b) Correlated.

Fig. 10. Scatter plots showing data samples of minimum creep rate (at an arbitrary stress) and ductility data with a) no correlation and b) a postulated 0.8 correlation.

correlations between minimum creep rate versus ductility, and primary creep rate versus ductility were based on a small number of data subsets which had relatively small samples sizes (see Fig. 4). This was a consequence of only a portion of the available data (286 tests out of > 1400 tests) having the full creep curve recorded. Thus for the vast majority of the available data, minimum and primary creep rates were not calculated. Nevertheless, Fig. 4 still shows that some significant correlations do exist between the various parameters, not least at 550°C which is the closest temperature to the range of most interest.

Two measures of ductility were examined: the last recorded inelastic strain and the percentage reduction of area. Both are uncertain

experimental results which attempt to measure uniaxial ductility. Fig. 5 shows Pearson correlations results between these two measures based on 25 data subsets, each having a sample size of at least 10 data points. The Pearson correlation is used in this instance to prove that the two parameters are proportional (i.e. linearly correlated). The results show that ϵ_{LS} and PRA are in fact strongly correlated which essentially implies that they are both proportional to the same quantity (i.e. ductility). For the closest temperature to plant operating temperatures (600°C) the correlations are consistently strong. Therefore, correlations between each of these two parameters and average creep rate can together provide enough quantitative evidence for the correlation of

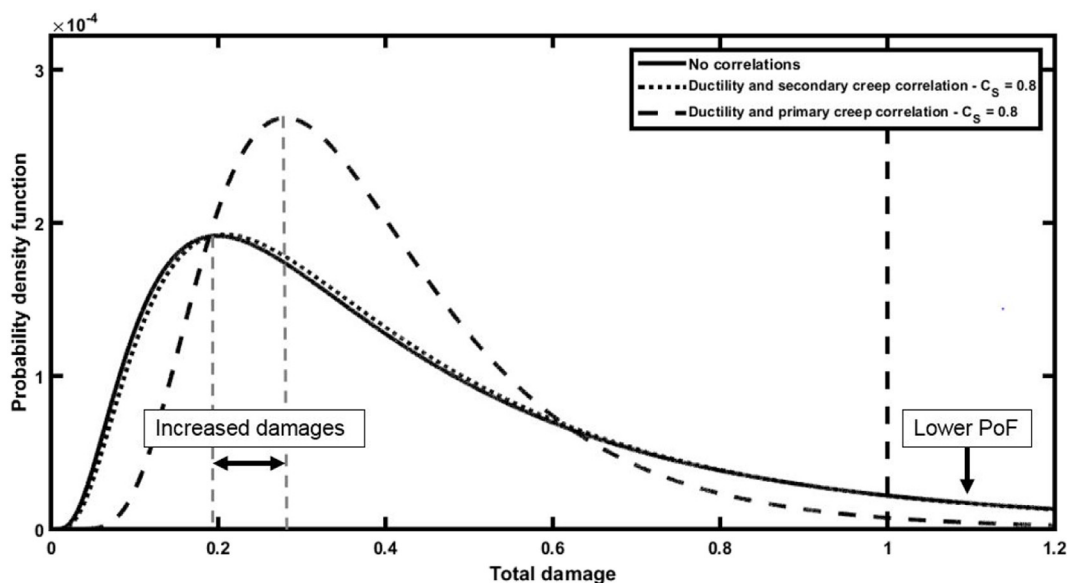


Fig. 11. Probabilistic results for uniaxial test specimen under creep-fatigue conditions showing the effects of correlations between creep parameters.

Table 2

Summary of statistical measures for comparing the correlated and uncorrelated results in Fig. 11.

Test statistic	Result
Mann-Whitney test	Null hypothesis upheld (medians are equivalent)
Quotion test	48.5%
F-test	Variances of logarithms are not equivalent
Brown Forsythe's test	Variances are not equivalent
Probability of failure	Uncorrelated: 9.6% Correlated: 1.4%

interest. The set of two correlation results are shown in Fig. 6. Each plot in Fig. 6 was based on 25 data subsets, each having a sample size of at least 10 data points, for which enough information was available to calculate the average creep rate.

Note that the results at 550°C were not included because that subset had a sample size less than 10 data points. Furthermore it is worth noting that the testing matrix is biased towards higher stresses and temperatures. This is due to the requirement for accelerated creep testing, which is a limitation of current creep testing efforts. To compromise between practicality and cost on the one hand and producing

results at conditions closer to the those of interest, higher stresses and temperatures are used in experiments. Using accelerated creep testing results for predicting plant material behaviour is considered an epistemic uncertainty, which is a major area of research. However, the results shown in Fig. 4 indicate that correlations at the same temperature but different stresses (see the results for 750°C) do not show a clear stress dependency. This was also the case for the results shown in Fig. 6a–b. Stress or temperature dependencies were not, therefore, identified as they may have been effectively masked by the significant variability in the correlation results.

Nevertheless, the results in Fig. 6 exhibit a significant positive correlation does exist, and histograms of these results are presented in Fig. 6. The normal distribution and the Minimum Extreme Value Type I distributions were found to best represent the histograms in Fig. 7. The normal distribution is described by the following PDF:

$$f(C_S) = \frac{1}{\sigma_{SD} \sqrt{2\pi}} \exp \left[-\frac{(C_S - \mu)^2}{2\sigma_{SD}^2} \right] \tag{5}$$

where C_S is the Spearman correlation, μ is the mean and σ_{SD} is the standard deviation. By contrast, the PDF for the Minimum Extreme Value distribution is:

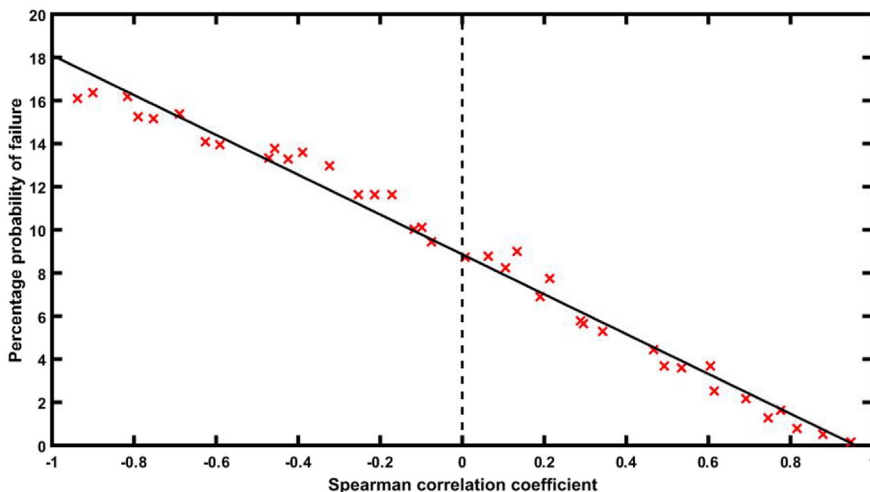


Fig. 12. Probability of failure calculated based on the results from probabilistic assessments incorporating the full range of correlation coefficients between K and ϵ_f .

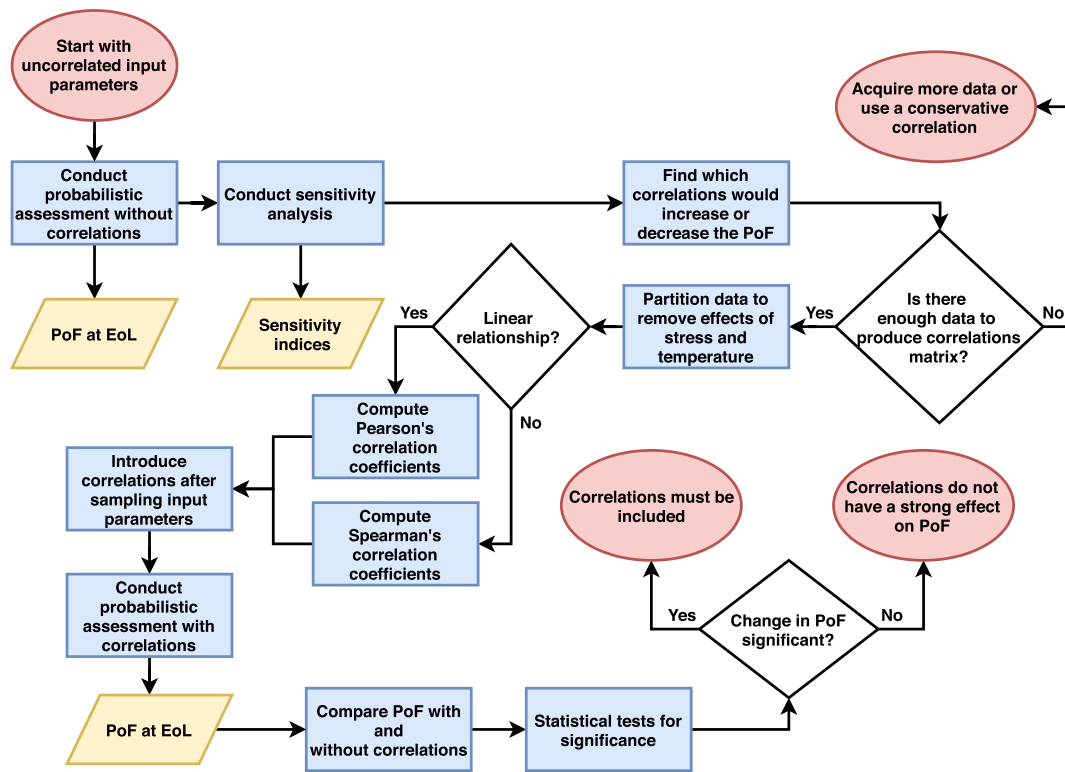


Fig. 13. Proposed procedure for assessing the importance of input parameter correlations in probabilistic creep assessments.

$$f(C_s) = \frac{1}{\theta} \exp \left[\frac{C_s - \nu}{\theta} - \exp \left(\frac{C_s - \nu}{\theta} \right) \right] \quad (6)$$

where θ and ν are the scale and location parameters respectively. A summary of the parameters calculated from fitting these two distribution types to the histograms shown in Fig. 7 is provided in Table 1.

For a creep damage assessment based on creep rupture time (e.g. using a time fraction rule) instead of ductility, the required correlation is between scatter in creep rupture time and creep deformation. Fig. 8 shows correlations between average creep rate and creep rupture time. The two parameters are negatively correlated and a stress dependency can be observed, as lower stresses seems to exhibit lower correlation values. As this work is more focused on ductility based creep damage assessments, the effects that this correlation might have on the probabilistic results of a rupture time based assessment were not explored and these results were only included for completeness.

Finally, Fig. 9 shows results for correlations between scatter in the creep rupture time and ductility. Some degree of stress dependency is observed with somewhat weak positive correlations at lower stresses and even weaker (often negative) correlations for higher stresses. However, due to the nature of creep damage assessments, creep rupture and creep damage caused by deformation are decoupled, which is the case in the R5 Volume 2/3 [5] assessment procedure. Therefore, although insightful, these correlations are not directly applicable to such creep crack initiation assessments. These results may be relevant for probabilistic assessments which assess creep crack initiation and creep rupture in parallel, in which case a correlation between ductility and rupture time is applicable.

4. Implications for probabilistic assessment results

Fig. 10a shows a scatter plot for two creep parameters which are assumed to be statistically independent. Without a correlation between the scatters in the properties two overly populated regions exist in the plot (referred to as regions of atypical behaviours in Fig. 10a). In this context atypical means relatively infrequent, but without a correlation

these samples are as frequent as the more typical samples. The effect of excluding correlations is to effectively increase the overall uncertainty in the probabilistic results, a measure of which is the width of the output parameter PDF (see Fig. 11 as an example). Incorporating correlations has the effect of reducing the number of samples in these atypical regions as shown in Fig. 10b.

Fig. 11 shows probabilistic results for a creep-fatigue initiation assessment of a uniaxial specimen. This probabilistic creep-fatigue assessment used the RCC-MR creep deformation model and stress independent ductility exhaustion for the calculation of creep damage. The details of this probabilistic assessment can be found in Ref. [15]. Incorporating a positive correlation between uniaxial ductility and the primary creep rate had a significant effect by reducing the overall uncertainty in the results. On the other hand, the postulated 0.8 correlation between ductility and secondary creep rate had virtually no effect. This can be explained in light of previous work in which this probabilistic assessment was subject to four types of sensitivity analysis techniques [15]. All four analyses indicated that the secondary creep rate had a marginal effect on the probabilistic results, whilst the primary creep rate and ductility dominated. Thus the effects shown in Fig. 11 indicate that correlations have a significant effect on the assessment results only if both parameters have a strong degree of influence.

To quantify the effects that incorporating a correlation has on the results of a probabilistic assessment, a number of approaches were suggested:

1. The Mann-Whitney test [16] (also known as the Wilcoxon rank sum test) which tests the null hypothesis that the two sets of results are sampled from two continuous distributions with equal medians, against the alternative that they are not. By using the left-tailed hypothesis version, this establishes whether correlations cause a significant increase in predicted damage by comparing the medians of the PDFs.
2. The Quotion test [17] which measures the probability of increasing

the overall damage (i.e. shifting the PDF to the right) by introducing a correlation relative to the uncorrelated case. This is defined as:

$$P_{\text{shift}} = p\left(\frac{D_{\text{Corr}}}{D} \geq 1\right) \quad (7)$$

where D and D_{Corr} denote sets of random samples from the distributions of uncorrelated and correlated results respectively. If absolutely no effect exists, then P_{shift} should be close to 0.5. This would in essence mean that the probability of achieving a PDF shift to the right is equal to that of a left shift, and thus no clear effect can be deduced.

3. The F-test which compares two data sets in terms of their variances. This test only applies to data sets which are normally distributed and thus can be somewhat restrictive. However, noting that the PDFs in Fig. 11 were lognormal, the logarithm of the results can be treated as normal, rendering the F-test applicable.
4. The Brown-Forsythe's test [18,19] which is an equivalent to the F-test but remains robust for non-normally distributed data. This relies on firstly transforming the data sets using their respective medians, for example:

$$z = |D - \tilde{D}| \quad (8)$$

where D denotes the results obtained from a probabilistic assessment using uncorrelated parameters, and \tilde{D} is the associated median. Thereafter an F-test is performed on the two transformed sets of results for the equivalence of their variances (i.e whether the two sets of results are *homoscedastic*).

5. The probability of failure defined as:

$$P_f = \int_1^{\text{inf}} f(D)dD \quad (9)$$

These five measures were calculated for the results shown in Fig. 11 to examine the effects of a postulated 80% positive correlation between primary creep rate and ductility. The results are summarised in Table 2. These results indicate that no significant shift of the PDF was observed as the Mann-Whitney test showed that the median was not significantly affected, whilst the Quotion Rule yielded a result very close to 50%. Effects on predicted damages notwithstanding, the F-test and Brown-Forsythe's test indicated that this correlation had a significant effect on the variance, which in effect is a measure of uncertainty or dispersion in the results. More importantly, the correlation had a significant effect on the predicted PoF, which is often the most crucial outcome of a probabilistic assessment. Therefore, the key benefit of incorporating a positive correlation is reducing the area between the right hand tail of the distribution and the line demarking the failure criterion (in this case a damage equal to unity). Therefore reducing the predicted PoF. This effect is further highlighted in Fig. 12 which shows that for the probabilistic assessment being considered [15], there is a linear relation between the predicted PoF and the postulated correlation coefficient.

Finally, Fig. 13 shows a proposed procedure for firstly assessing the importance of incorporating a possible correlation between input parameters, then calculating this correlation based on partitioned data sets and thereafter incorporating this correlation at the sampling stage during a probabilistic assessment. The main output of a probabilistic assessment is assumed to be the PoF at the end of life (EoL). The procedure does rely on conducting a sensitivity analysis to establish which input parameters dominate the results of the probabilistic assessment. In the absence of adequate data sets, a postulated range of correlations can still be trialled and for a given probabilistic assessment a plot equivalent to the one shown in Fig. 12 can be produced. Such a plot can assist in making a judgement as to what an adequate correlation could be in the absence of experimental evidence to characterise such correlation. Indeed even when some data is available, the sought correlation might still be uncertain (for example following a distribution like the one shown in Fig. 7), in which case trialling a range of possible

correlations to examine their effect on the PoF would aid judgement.

5. Conclusions

Key parameters involved in creep damage assessments can be correlated, with these correlations being an additional uncertainty to the scatter in the parameter data. Incorporating these correlations typically has the effect of reducing the overall uncertainty in the output results, and can have a major effect on the predicted PoF. However, due to limited data sets and large variability, these correlations remain uncertain. They can still be accommodated in probabilistic assessments by treating them stochastically according to the available results.

Uncertain knowledge of any possible correlations does not preclude conducting a probabilistic assessment. Rather a probabilistic assessment using uncorrelated parameters in conjunction with post-assessment sensitivity analyses can provide insights into which inter-parameter correlations would have a marked effect. Sensitivity analysis is therefore advised as a precursor to any investigation into possible correlations, thus providing focus for reducing uncertainties in the assessment results.

Significant positive correlations were found between scatter in creep ductility and creep deformation parameters, which are two of the main material properties required for creep damage calculations in R5 Volume 2/3 assessments. These represent cast-to-cast correlations, which dominate the variabilities in creep properties. The Spearman correlation was deemed appropriate for such applications, as it does not impose any restrictions on the distributions of the correlated parameters and can be used for parameters following different distribution types. Thus it provides a simple and flexible way of incorporating correlations in probabilistic assessments. For a creep crack initiation probabilistic assessment, the inclusion of a positive correlation between creep deformation and ductility will lead to reduced probabilities of failure being predicted, as compared with ignoring such correlation.

Acknowledgment

The authors would like to express their gratitude for the support of EDF Energy towards this project and in particular Marc Chevalier and Phil Cairns.

References

- [1] M.J. Chevalier, The Reliability of Degrading Structural Systems Operating at High Temperature, Ph.D. thesis University of Bristol, 2013 Mar.
- [2] R. Bradford, P. Holt, Application of probabilistic modelling to the lifetime management of nuclear boilers in the creep regime: Part 2, Int. J. of Pressure Vessels & Piping 111–112 (2013) 232–245.
- [3] T.J. Delph, D.L. Berger, D.G. Harlow, M. Ozturk, A probabilistic lifetime prediction technique for piping under creep conditions, J. Pressure Vessel Technol. 132 (5) (2010) 051206–051206.
- [4] B. Dogan, U. Ceyhan, J. Korous, F. Mueller, R. Ainsworth, Sources of scatter in creep-fatigue crack growth testing and their impact on plant assessment, Weld. World 51 (7) (2007) 35–46.
- [5] D.W. Dean, P.J. Budden, R.A. Ainsworth, R5 procedures for assessing the high temperature response of structures: current status and future developments, Proceedings of ASME PVP2007, Texas, USA, paper PVP2007-26569, San Antonio, July 22–26, 2007.
- [6] AFCEM, RCC-MR, Design and Construction Rules for Mechanical Components of FBR Nuclear Islands, (1985).
- [7] A. Mehmanparast, C.M. Davies, G.A. Webster, K.M. Nikbin, Creep crack growth rate predictions in 316h steel using stress dependent creep ductility, Mater. A. T. High. Temp. 31 (1) (2014) 84–94.
- [8] J.D. Booker, M. Raines, K.G. Swift, Designing Capable and Reliable Products, Butterworth-Heinemann, 2001.
- [9] D.C. Montgomery, G.C. Runger, Applied Statistics and Probability for Engineers, John Wiley and Sons, 2003.
- [10] Y.M. Goh, The Incorporation of Uncertainty into Engineering Knowledge Management, Ph.D. thesis University of Bristol, Jan. 2005.
- [11] M.C. Cario, B.L. Nelson, Modelling and Generating Random Vectors with Arbitrary Marginal Distributions and Correlation Matrix, Tech. Rep, Delphi Packard Electric Systems (Warren, OH) and Department of Industrial Engineering and Management Science, Northwestern University (Evanston, IL), 1997.
- [12] Matworks, Generate correlated data using rank correlation, <https://uk.mathworks>.

- [com/help/stats/generate-correlated-data-using-rank-correlation.html](https://uk.mathworks.com/help/stats/generate-correlated-data-using-rank-correlation.html), (2017) , Accessed date: 30 May 2017.
- [13] M. W. Spindler, M. C. Smith, The effect of multiaxial states of stress on creep failure of type 316h under displacement control. Proceedings of ASME PVP2009, July 26–30, 2009, Prague, Czech Republic, paper PVP2009-77963.
- [14] British Steelmakers Creep Committee, BSCC High Temperature Data: British Long Term Creep Rupture and Elevated Temperature Tensile Data on Steels for High Temperature Service, Iron and Steel Institute for the British Steelmakers Creep Committee, London, 1973.
- [15] N.A. Zentuti, J.D. Booker, R.A.W. Bradford, C.E. Truman, A review of probabilistic techniques: towards developing a probabilistic lifetime methodology in the creep regime, *Mater. A. T. High. Temp.* 34 (5–6) (2017) 333–341.
- [16] Matworks, Wilcoxon rank sum test: ranksum, <https://uk.mathworks.com/help/stats/ranksum.html>, (2017) , Accessed date: 19 June 2017.
- [17] D.J. Smith, J.D. Booker, Statistical analysis of the effects of prior load on fracture, *Eng. Fract. Mech.* 14 (74) (2007) 2148–2167.
- [18] M.B. Brown, A.B. Forsythe, Robust tests for the equality of variances, *J. Am. Stat. Assoc.* 69 (346) (1974) 364–367.
- [19] A. Trujillo-Ortiz, R. Hernandez-Walls, Bftest: Brown-Forsythe's test for homogeneity of variances, a MATLAB® file, <http://www.mathworks.com/matlabcentral/fileexchange/loadFile.do?objectId=3412&objectType=FILE>, (2003) , Accessed date: 19 June 2017.